R. S. Cumbee is with University of Maryland, College Park, MD 20742 but due to publisher's guidelines you are unable to make changes at this point.

Optimization of X-ray Absorbers for High-Resolution TES Detectors in NewATHENA X-IFU

T. Farrahi, E. J. Wassell, J. S. Adams, C. V. Ambarish, S. R. Bandler, R. B. Borrelli, J. A. Chervenak, F. A. Colazo Petit, R. S. Cumbee, N. S. DeNigris, F. M. Finkbeiner, J. D. Fuhrman, S. V. Hull, R. L. Kelley, C. A. Kilbourne, H. Muramatsu, F. S. Porter, A. Rani, K. Sakai, S. J. Smith, N. A. Wakeham, M. C. Witthoeft, S. H. Yoon

***Abstract*—NewATHENA's X-ray Integral Field Unit (X-IFU) uses a large-format array of Transition Edge Sensor (TES) microcalorimeters coupled with absorbers made of gold and bismuth providing 4 eV FWHM resolution up to 7 keV in the 0.2-12 keV band. X-ray absorbers must be thick enough for photon absorption, maintain low heat capacity for energy resolution, and have good thermalization properties. The X-IFU requires total Quantum Efficiency (QE) of 96%, 87%, and 63% at 1, 7, and 9.5 keV, respectively. Optimal thicknesses are 1.05 μm gold and 5.5 μm bismuth to achieve 0.731 pJ/K at 90 mK and 87% QE at 7 keV. While typical TES absorbers are 3-4 μm thick, producing the required 5.5 μm Bi absorbers via standard electroplating creates enlarged grains and surface roughness. The increased roughness and grain size variability produced with our standard recipe have resulted in instances of 1) low energy spectral tails 2) spectral broadening of the energy resolution and 3) thermal shorts between pixels when a large grain bridges the gap between absorbers. In this study, we have introduced a new fabrication process and altered the morphology of the thick Bi through changes in the electroplating process. The process changes are intended to address all three issues as well as reduce particulate contamination observed on the finished detector arrays.**

***Index Terms*—Absorber, bismuth, electroplating, X-ray, TES detectors, PVA**

I. Introduction

THE new Advanced Telescope for High Energy Astrophysics (ATHENA), ESA's flagship X-ray astronomy mission, is set to deliver unprecedented spectroscopic capabilities for studying the hot and energetic universe [1]. NewATHENA's X-ray Integral Field Unit (X-IFU) employs large-format arrays of Transition Edge Sensor (TES) microcalorimeters to achieve an energy resolution of 4 eV FWHM up to 7 keV across the 0.2-12 keV soft X-ray band, which implies much better performance at the detector and absorber levels. The TES is coupled to a Ti/Au/Bi/Au absorber that provides not only the X-ray stopping power [2]–[4], but also dominates the total heat capacity and provides reflectivity for longer wavelength photons [5]. Bismuth's properties, such as low specific heat capacity and X-ray stopping power, have made it an excellent choice for the absorber material of TES arrays [6], [7]. Bismuth can be deposited both by evaporation and electroplating. Studies show that TES detectors with electroplated bismuth have eliminated non-Gaussian low-energy spectral tails that might be caused by the trapping of energy in the grain boundaries of fine-grained evaporated films (∼1-3 μm versus ∼30 nm) [8]–[10]. The larger grain structure (1-10 μm) is expected to improve the thermalization of the secondary electron cloud generated by incident X-rays because the cloud interacts with fewer grain boundaries, reducing the number of incomplete energy collection events [11], [12].

The total Quantum Efficiency (QE) requirements for X-IFU are currently 96%, 87% and 63% at 1, 7, and 9.5 keV, respectively. Historically, our group at NASA has demonstrated TES microcalorimeter absorbers with a 2 μm Au layer and a 3.75 μm Bi layer. These pixels had a pitch of 275 μm. To achieve vertical QE (absorption quantum efficiency along the vertical cross-section of a detector) $>$ 90.6% at 7 keV and the required heat capacity of 0.731 pJ/K at 90 mK operating temperature, changes in the fabrication process are required: transitioning to 1.0 μm Au layer and 5.5 μm Bi layer. The most recent X-IFU array requirements specify pixels with a 317 μm pitch and 5 μm gap between pixels. Decreasing the gap between absorbers with completely vertical sidewalls is essential for increasing uniform quantum efficiency. Scaling bismuth electroplating from prototypical 3-4 μm thicknesses to the required 5.5 μm may cause unwanted film characteristics such as coarsened microstructure, elevated surface roughness, and runaway grain growth, resulting in thermal cross-talk between pixels [13], which in turn may lead to detector behaviors, significant secondary time constants in the X-ray pulses, the presence of low energy spectra, and energy resolution degradation [10]. The roughening and runaway issues lead to fabrication challenges that may be tackled with a refinement of the

Corresponding author: T. Farrahi, e-mail: tannaz.farrahi@nasa.gov
T. Farrahi and M. C. Witthoeft are with ADNET Systems LLC, 66720B Rockledge Drive, Suite 504 Bethesda, MD 20817
J. S. Adams, J. D. Fuhrman, N. A. Wakeham, and K. Sakai are with Center for Space Sciences and Technology, University of Maryland, Baltimore County, Baltimore, MD 21250
C. V. Ambarish, and S. V. Hull are with University of Maryland, College Park, MD 20742
H. Muramatsu is with Catholic University of America, 620 Michigan Ave NE, Washington, DC 20064.
F. A. Colazo Petit is with Teltrium Inc., 6406 Ivy Lane, Suite 210. Greenbelt, MD 20770
F. M. Finkbeiner is with Sigma Space Corp. / Hexagon US Federal, 4600 Forbes Blvd., Lanham, MD 20706
A. Rani is with the Newton LLC, 5650 Rivertech Ct suite A, Riverdale, MD 20737
S. H. Yoon is with the Columbus Technologies and Services, Inc., 7500 Greenway Center Drive, 16th Floor, Greenbelt, Maryland 20770
All the authors above are also with NASA Goddard Space Flight Center (GSFC), Greenbelt, MD 20771, USA.
S. R. Bandler, R. B. Borrelli, J. A. Chervenak, R. S. Cumbee, N. S. DeNigris, R. L. Kelley, C. A. Kilbourne, F. S. Porter, S. J. Smith, and E. J. Wassell are with NASA Goddard Space Flight Center (GSFC), Greenbelt, MD 20771, USA

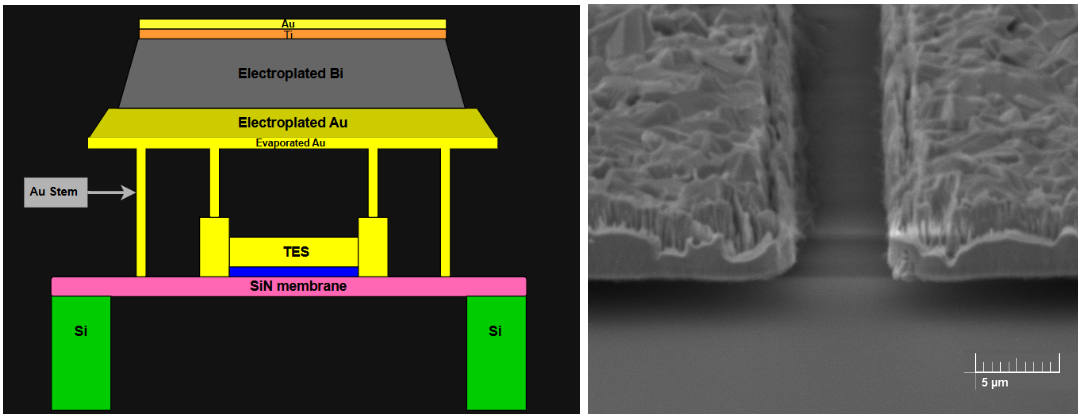

Fig. 1: **Right)**: Schematic of a TES pixel cross-section depicting an X-ray absorber thermally linked to the sensor via thin stems and suspended above a low-conductance SiN membrane, and **left)**: SEM of the edge of Bi absorber after ion mill.

grain size during electrodeposition. Grain uniformity may also lead to improved film thermal performance by reducing the population of smaller grains surrounding large-grains.

In this paper, we address these issues by reporting on Bi electroplating recipe optimization through the incorporation of polyvinyl alcohol (PVA) as a grain refining additive. We have previously reported high quality Bi film growth for this application as modified from other recipes [14]–[16]. While our attempts to optimize the grain size and grain uniformity using the old recipe by applying systematic variations in current density and pulse width parameters yielded no significant improvements, the addition of PVA demonstrated a significant reduction in grain size and improved grain uniformity. Optimal concentrations of PVA were determined utilizing confocal interferometry for different growth conditions. The optimized methodology produces mechanically robust and free-standing absorbers that could potentially preserve the required heat capacity while eliminating energy resolution degradation and spectral artifacts.

Our previously reported fabrication technique [5] uses ion milling of the entire Au/Bi stack, which becomes problematic for thick bismuth films, where the presence of significantly large grains and enhanced roughness leads to metal bridging during extended milling processes, creating thermal shorts between adjacent pixels that degrade the energy resolution of TES detector arrays. In our previous work [16], we reported on the formation of Bi absorbers using a photoresist mold followed by an ion mill to clear the streets of the seed Ti/Au. Our initial results showed thickness variations across the wafer and within the arrays, as well as wider gaps between pixels than required for an optimal fill factor. In this study, we present an optimization of the photoresist mold process to improve the thickness uniformity of the pixels and reduce the effective gaps between absorber pixels, with the goal of improving the QE of detectors while meeting other project specifications.

II. Absorber Design Optimization

The NewATHENA X-IFU transition edge sensors use free-standing absorber structures with six narrow gold-filled stems (4-5 μm diameter) supporting 317 μm^2 absorbers on a Ti/Au seed bilayer. As shown in Figure 1, each absorber consists of a 1.05 μm gold layer beneath 5.5 μm of bismuth, with a thin Ti/Au capping layer. We electroplate bismuth through photoresist molds, which significantly reduces the ion mill time needed to clear only the Ti/Au seed and capping layers between pixels. The mask used to form the photoresist mold consists of the main and witness arrays, as shown in Figure 2, where the main array has 7 μm line widths and witness pixels have 10 μm line widths. It should be noted that the photoresist (PR) mold, while having the potential to improve the QE and uniformity, does have an issue with local current density increase in regions where the pattern is isolated and smaller than a few millimeters, causing the thickness to vary over that distance. We counter this unwanted effect with an

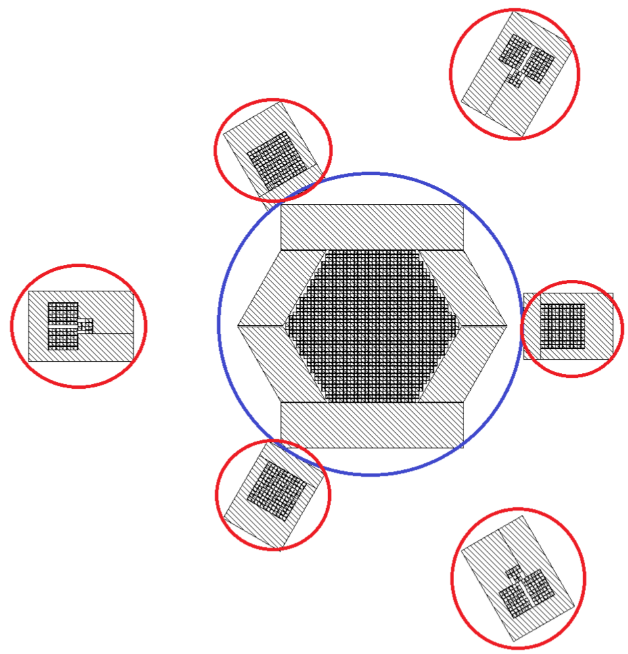

Fig. 2: Schematic layout of the TES detector array with the main and witness arrays highlighted in blue and red circles, respectively.

TABLE I: As designed and measured PR mold and hood gap widths for main and witness pixel arrays.

As designed mold (μm)/ hood (μm)	Average measured (μm)	Standard deviation (μm)	Average Au/Bi step width (μm)
7 / 7 - Main array	4.648/7.519	0.222/0.176	1.435
10 / 6 - witness array	2.978/9.286	0.383/0.375	2.709
10 / 5 - witness array	2.527/9.053	0.272/0.209	3.347
10 / 4 - witness array	2.129/8.904	0.181/0.404	3.352

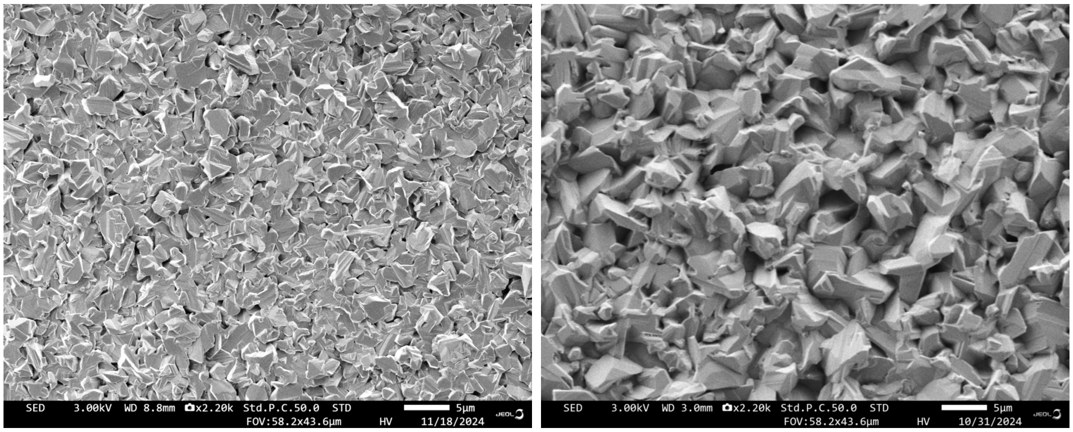

Fig. 3: **Left)** SEM of 3 μm thick bismuth film and **right)** 5.5 μm thick Bi film using the current newATHENA recipe prior to the addition of PVA.

added suitable width of buffer regions to surround any feature with critical thickness requirements. While critical thicknesses can be met for pixels within the main array and for witness pixels far from the array, an additional fabrication challenge of removing the buffer features cleanly arises.

In the fabrication of TES absorbers, we use a sacrificial photoresist underneath the absorbers. After the addition of the Ti/Au seed layer and electroplated Au layer, to avoid reflow in the underlying photoresist, we tend to underbake the PR mold, which results in the loss of some line width during development. Table I. details our design specs and measurements. In the main array, the measured gap distance between adjacent absorbers is slightly less than 5 μm, and this value for witness pixels is around 9 μm. After bismuth electroplating and removing the PR mold, the wafer is repatterned with a hood mask designed to clear the Au streets between pixels. Because the resist pools in the gaps between pixels, this layer needs overexposure to clear the resist so that the ion mill can etch the Au. This overexposure effectively widens the width of the gaps in the mask. Geometrically, the ion beam must traverse 3 μm of photoresist and 6 μm of bismuth in the effective gap to etch the Au between streets. Therefore, we designed an experiment with different gap widths in the hood mask to examine whether the ion beam can clear the designed streets with different widths. The average designed and measured gap widths between adjacent pixels of the main and witness arrays are listed in Table 1. In the main array, the gap width at the edge of the absorbers has widened to $\sim$ 7.5 μm. In the witness arrays, no bismuth is etched. The 4 μm hood gap resulted in slightly more than 2 μm of separation between absorbers, and the 6 μm hood gap had slightly less than 3 μm of separation. This result seems to suggest that there are more opportunities to further improve the total fill factor of the array.

III. ABSORBER MATERIAL OPTIMIZATION

Increasing bismuth electroplating thickness to the required 5.5 μm, as shown in Figure 3 and reported by other groups [14], [15], may be related to detector behaviors such as coarsened microstructure, elevated surface roughness, and runaway grain growth. To reduce the grain size, grain non-uniformity, and surface roughness of the absorber and minimize low-energy tails in the histogram of X-ray spectral response to monoenergetic deposition, bismuth films were fabricated using an optimized electroplating approach. Our previously reported standard bismuth electroplating solution incorporated betaine as a grain refiner in the electrolyte solution. In this study, we investigated incorporating polyvinyl alcohol (PVA) in addition to citric acid as a grain refiner, as reported by other groups [17], replacing the standard betaine additive in our electrolyte solution. The electroplating was conducted on a 200 nm evaporated Au and 800 nm pulsed electroplated Au seed layer on 4-inch Si/SiO_2 wafers at room temperature with no agitation in a vertical orientation, with a maintained 3 cm separation between anode and cathode to ensure uniform electric field distribution. Using optimized parameters of 2.16 mA/cm^2 current density and 10% forward pulse duty cycle, we successfully achieved the target thickness of 5.5 μm within a 1-hour deposition period. Film thickness was determined through differential weight measurements before and after electroplating for the growth area.

In a series of experiments, we studied the effect of I) PVA concentration, ii) current density, iii) pulse duty cycle, and iv) PVA hydrolyzation percentage on the grain size and surface roughness of 5.5 μm thick Bi films. The averaged surface roughness values obtained from the center and edge of wafers using a Keyence VK-X3000 laser confocal microscope. As depicted in Figure 4, investigating different concentrations

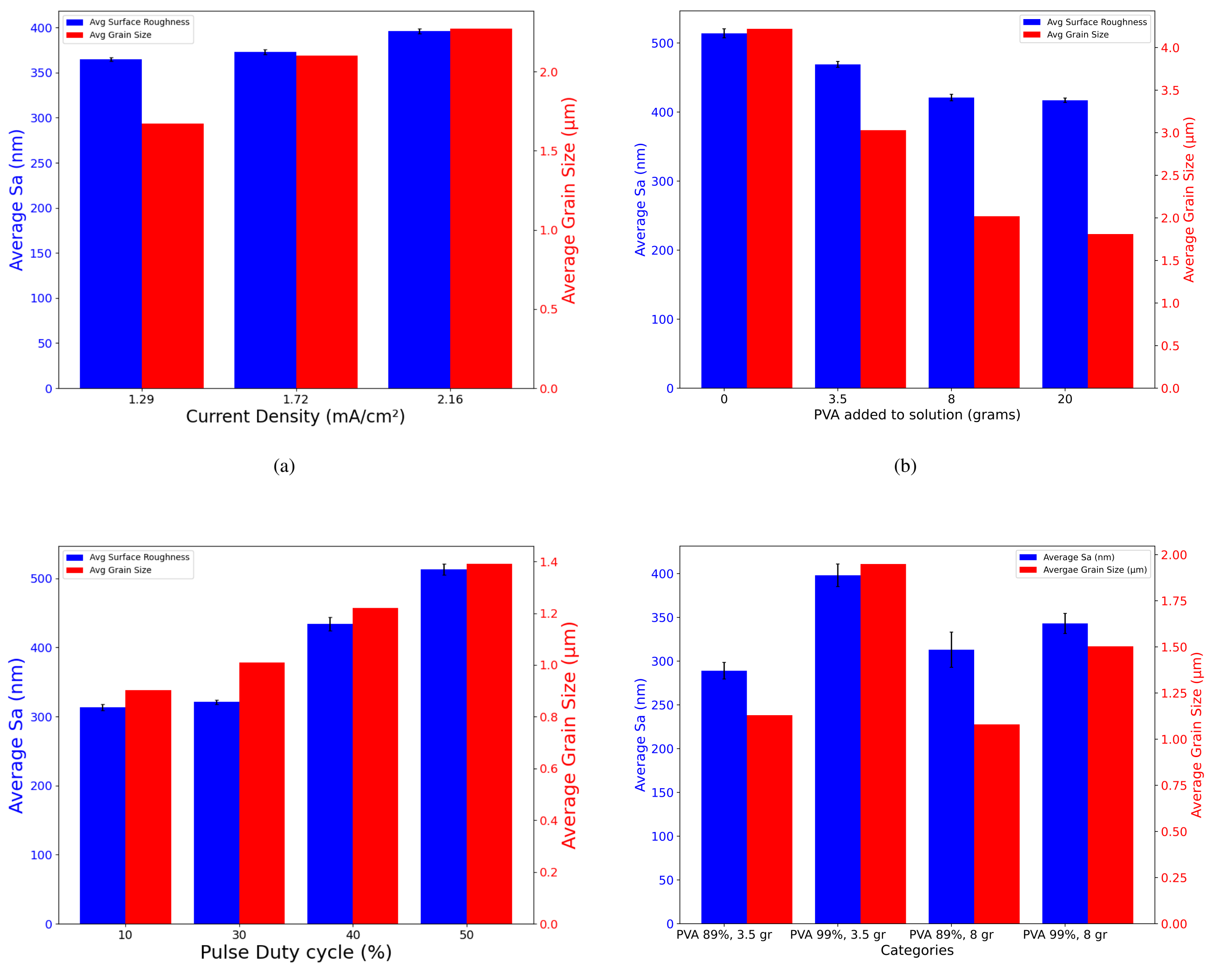

(a) (b) (c) (d)

Fig. 4: Average surface roughness and grain size of 5.5 μm thick Bi films at the center of the wafer as (a) a function of current density grown with 13 grams of PVA (99% hydrolyzed) and no betaine, (b) a function of PVA (99% hydrolyzed) added to the solution using 3 grams of betaine and current density of 2.16 mA/cm^2, (c) a function of pulse duty cycle using 8 grams of 89% hydrolyzed PVA and no betaine with 2.16 mA/cm^2 current density, and (d) comparison of the effect of 89% and 99% hydrolyzed PVA on surface roughness (center of wafer) and grain size of 5.5 μm electroplated Bi films.

of 99% hydrolyzed PVA, we found that a minimum of 8 grams of PVA is required to achieve notable improvement in grain size and surface roughness of Bi films. Increasing pulse duty cycle and current density resulted in the growth of larger Bi grains and rougher surfaces. When using 99% hydrolyzed PVA, we achieved improvements with grain size reductions ranging from 28-56% and surface roughness reductions of 8-18%. Figure 5 shows the thickness profile of a 48-pixel absorber array electroplated using 16 grams of 99% hydrolyzed PVA. The measured absorber thickness was 5.9 μm at the center with a standard deviation of 0.455 indicating minimal variation of Bi thickness across the array. While this approach provided the benefits mentioned above, it also created drawbacks such as undesirable streaking (non homogeneous growth) patterns across the film surface and multilayer grain structures similar to the grain structure of evaporated Bi films that could compromise detector performance. The multilayered grain morphology creates significantly higher thermal resistance and phonon scattering rates and consequently limits vertical heat transport that is critical for optimal TES operation. Streaking patterns mainly originate from the residual particles of 99% hydrolyzed PVA as this variant shows insufficient solubility in the cold electrolyte solution. Our investigation shows that PVA hydrolyzation percentage dramatically affects the properties of bismuth films. It is reported that PVA with 87-89% hydrolysis has better cold-solution compatibility [18]. Analysis of grain size for the films electroplated using 89% PVA variant demonstrated that

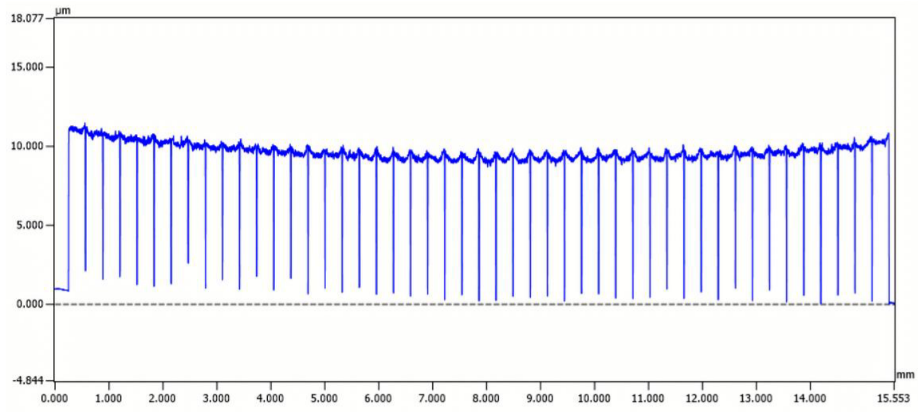

Fig. 5: Absorber thickness distribution of a 48-pixel section across a $\sim$ 1.5 kilo-pixel array is shown from edge to edge. Absorbers were electroplated with targeted 5.9 μm thick Bi. Measured standard deviation of 0.455 indicating minimal variation across these pixels.

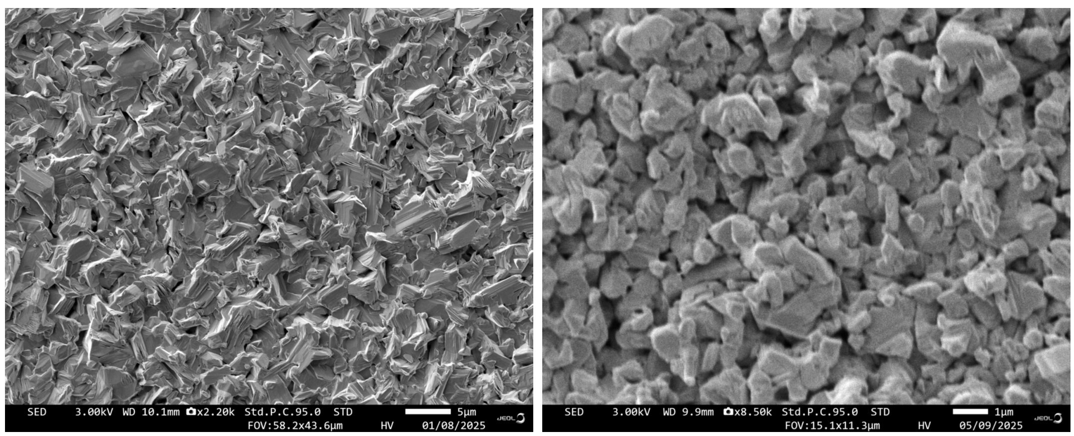

Fig. 6: **Left)** SEM image of 5.5 μm thick Bi with 99% hydrolyzed PVA and **right)** 89% hydrolyzed PVA.

substituting 3.5 grams of 89% hydrolyzed PVA for the 99% variant resulted in an average Bi grain size reduction from 1.94 μm to 1.12 μm. Corresponding surface roughness analysis indicated 27.4% improvement at the center of the wafer. The less hydrolyzed formulation of PVA grain refiner maintained the beneficial grain structure of Bi films similar to our pre-refinement baseline conditions, while still achieving significant grain size reduction and producing notably smoother surface morphology and more uniform grain structure. Importantly, 89% hydrolyzed PVA completely resolved the streaking issues caused by PVA salt deposits on the film surface and eliminated the multilayer grain structure, as shown in Figure 6.

IV. CONCLUSION

In this study, we presented advances in the fabrication of thick bismuth absorbers for NewATHENA X-IFU TES detectors through design modifications and optimized electroplating processes. With the refined photoresist mold process and hood mask design, we achieved slightly below 5 μm absorber pixel separation with minimized Au/Bi step widths at the absorber edges. Scaling bismuth thickness to the required 5.5 μm resulted in significant grain coarsening and performance issues, which our initial implementation using 99% hydrolyzed PVA successfully addressed these issues by achieving grain size reductions of 28-56% and surface roughness improvements of 8-18%. However, this variant introduced problematic streaking patterns and multilayer grain structures that were successfully resolved by transitioning to 89% hydrolyzed PVA while maintaining superior grain control. This new 89% hydrolyzed PVA-based recipe has been incorporated into the full fabrication process as a drop-in replacement, enabling increased fill factor through improved sidewall control.

These fabrication improvements effectively mitigate thermal crosstalk between pixels while preserving the target grain size and surface roughness characteristics of the proven 3.8 μm films that performed well with previous recipes. The results demonstrate significant progress toward meeting NewATHENA X-IFU's stringent requirements for quantum efficiency and energy resolution. In Future studies, we will fabricate TES detectors with absorbers produced using the new recipe and demonstrate their ability to achieve the required structural, thermal, and electrical properties. In addition, we will focus on further narrowing the gap between absorbers and implementing the developed bismuth electroplating recipe with the goal of enhancing detection efficiency and spatial resolution in the next generation of devices.

References

[1] K. Nandra, D. Barret, X. Barcons, A. Fabian, J. Herder, L. Piro, M. Watson, C. Adami, J. Aird, J. Afonso, and D. Alexander, "The hot and energetic universe: A white paper presenting the science theme motivating the athena+ mission," *arXiv preprint arXiv:1306.2307*, 2013.

[2] P. Peille, D. Barret, E. Cucchetti, V. Albouys, L. Piro, A. Simionescu, M. Cappi, E. Bellouard, C. Cénac-Morthé, C. Daniel, and A. Pradines, "The x-ray integral field unit at the end of the athena reformulation phase," *Experimental Astronomy*, vol. 59, no. 2, pp. 1–36, 2025.

[3] D. Barret *et al.*, "The athena x-ray integral field unit: a consolidated design for the system requirement review of the preliminary definition phase," *Experimental Astronomy*, vol. 55, no. 2, pp. 373–426, 2023.

[4] S. Smith, J. Adams, S. Bandler, G. Betancourt-Martinez, J. Chervenak, M. Chiao, M. Eckart, F. Finkbeiner, R. Kelley, C. Kilbourne, and A. Miniussi, "Transition-edge sensor pixel parameter design of the microcalorimeter array for the x-ray integral field unit on athena," in *Space Telescopes and Instrumentation 2016: Ultraviolet to Gamma Ray*, vol. 9905. SPIE, 2016, pp. 772–790.

[5] R. Hummatov, J. Adams, S. Bandler, A. Barlis, S. Beaumont, M. Chang, J. Chervenak, A. Datesman, M. Eckart, F. Finkbeiner, and J. Ha, "Quantum efficiency study and reflectivity enhancement of au/bi absorbers," *Journal of Low Temperature Physics*, vol. 199, no. 1, pp. 393–400, 2020.

[6] N. Iyomoto, J. Sadleir, E. Figueroa-Feliciano, T. Saab, S. Bandler, C. Kilbourne, J. Chervenak, D. Talley, F. Finkbeiner, R. Brekosky, and M. Lindeman, "Optimization of x-ray absorbers for tes microcalorimeters," in *High-Energy Detectors in Astronomy*, vol. 5501. SPIE, 2004, pp. 145–154.

[7] S. Bandler, R. Brekosky, A. Brown, J. Chervenak, E. Figueroa-Feliciano, F. Finkbeiner, N. Iyomoto, R. Kelley, C. Kilbourne, F. Porter, and J. Sadleir, "Performance of tes x-ray microcalorimeters with a novel absorber design," *Journal of Low Temperature Physics*, vol. 151, no. 1, pp. 400–405, 2008.

[8] A. Brown, S. Bandler, R. Brekosky, J. Chervenak, E. Figueroa-Feliciano, F. Finkbeiner, N. Iyomoto, R. Kelley, C. Kilbourne, F. Porter, and S. Smith, "Absorber materials for transition-edge sensor x-ray microcalorimeters," *Journal of Low Temperature Physics*, vol. 151, no. 1, pp. 413–417, 2008.

[9] D. Yan, R. Divan, L. Gades, P. Kenesei, T. Madden, A. Miceli, J. Park, U. Patel, O. Quaranta, H. Sharma, and D. Bennett, "Eliminating the non-gaussian spectral response of x-ray absorbers for transition-edge sensors," *Applied Physics Letters*, vol. 111, no. 19, 2017.

[10] J. Weber, K. Morgan, D. Yan, C. Pappas, A. Wessels, G. O'Neil, D. Bennett, G. Hilton, D. Swetz, J. Ullom, and D. Schmidt, "Development of a transition-edge sensor bilayer process providing new modalities for critical temperature control," *Superconductor Science and Technology*, vol. 33, no. 11, p. 115002, 2020.

[11] D. Yan, R. Divan, L. Gades *et al.*, "Microstructure analysis of bismuth absorbers for transition-edge sensor x-ray microcalorimeters," *Journal of Low Temperature Physics*, vol. 193, pp. 225–230, 2018.

[12] L. Fàbrega, A. Camón, J. Costa-Krämer, C. Pobes, M. Parra-Borderías, I. Fernández-Martínez, R. Jáudenes, P. Cereceda, M. Ceballos, X. Barcons, and J. Sesé, "Towards mo/au based tes detectors for athena/x-ifu," in *Space Telescopes and Instrumentation 2014: Ultraviolet to Gamma Ray*, vol. 9144. SPIE, 2014, pp. 1690–1696.

[13] A. Miniussi, J. Adams, S. Bandler, S. Beaumont, M. Chang, J. Chervenak, F. Finkbeiner, J. Ha, R. Hummatov, R. Kelley, and C. Kilbourne, "Thermal crosstalk measurements and simulations for an x-ray microcalorimeter array," *Journal of Low Temperature Physics*, vol. 199, no. 3, pp. 663–671, 2020.

[14] E. Sandnes, M. Williams, U. Bertocci, M. Vaudin, and G. Stafford, "Electrodeposition of bismuth from nitric acid electrolyte," *Electrochimica Acta*, vol. 52, no. 21, pp. 6221–6228, 2007.

[15] L. Gades, T. Cecil, R. Divan, D. Schmidt, J. Ullom, T. Madden, D. Yan, and A. Miceli, "Development of thick electroplated bismuth absorbers for large collection area hard x-ray transition edge sensors," *IEEE Transactions on Applied Superconductivity*, vol. 27, no. 4, pp. 1–5, 2017.

[16] E. Wassell, J. Adams, S. Bandler, J. Chervenak, R. Cumbee, F. Finkbeiner, J. Fuhrman, S. Hull, R. Kelley, C. Kilbourne, and J. Mateo, "Microcalorimeter absorber optimization for athena and lem," *Journal of Low Temperature Physics*, vol. 216, no. 1, pp. 417–426, 2024.

[17] A. Rajamani, S. Jothi, M. Kumar, S. Srikaanth, M. Singh, G. Otero-Irurueta, D. Ramasamy, M. Datta, and M. Rangarajan, "Effects of additives on kinetics, morphologies and lead-sensing property of electrodeposited bismuth films," *The Journal of Physical Chemistry C*, vol. 120, no. 39, pp. 22 398–22 406, 2016.

[18] S. Aldrich, "Poly (vinyl alcohol) average mw 85,000-124,000, 87-89% hydrolyzed," https://www.sigmaaldrich.com/US/en/product/aldrich/363081, 363081 datasheet.